Simulation of Diffraction in periodic Media with a coupled Finite Element and Plane Wave Approach

M. Huber, J. Schöberl, A. Sinwel and S. Zaglmayr *

Abstract

The aim of this paper is to discuss simulation methods of diffraction of electromagnetic waves on biperiodic structures. The region with complicated structures is discretised by Nédélec Finite Elements. In the unbounded homogeneous regions above and below, a plane wave expansion containing the exact far-field pattern is applied. A consistent coupling is achieved by the method of Nitsche. By numerical experiments we investigate the speed of convergence depending on the mesh refinement, the element order and the number of evanescent waves.

1 Introduction

In this paper we consider the scattering of an electromagnetic wave at a periodic or biperiodic structure called grating. At a large distance above or below, the field essentially consists of a finite number of plane waves (or modes). The directions of these modes follow directly from the period of the grating [7, 27], but the computation of the corresponding intensities requires the solution of Maxwell's equations. Such diffraction gratings are widely used in physics. While in the past spectroscopy was the major application, there are many promising developments in optics nowadays, like antireflection surfaces, waveguide couplers or the EUV-technology, where gratings play an essential role. A nice introduction to the diffraction problem is given in the books of Petit [25] and Nevière & Popov [23]. In literature, there exists a large variety of numerical methods to solve such problems. In our paper paper we apply the finite element method (FEM), see also [1, 2, 4, 13, 31, 3, 28]. The structure is subdivided into simple elements, and the field is approximated by piecewise polynomials, satisfying continuity constraints across element interfaces. The FEM is most flexible in modeling complicated,

*The authors acknowledges support from the Austrian Science Foundation FWF within project grant Start Y-192, "hp-FEM: Fast Solvers and Adaptivity"

possibly curved geometries. In the rigorous coupled wave method (RCW), see [19, 18, 23], the domain is sliced into layers, and on each layer, the solution is expanded into plane waves. The special structure allows a fast application of the transfer operators. Further alternatives are finite-difference methods [22, 35, 25], integral equation methods [25, 26], the boundary variation method [8, 9] or the curvilinear coordinate method (C-method) [10, 15].
Bloch - Floquet theory allows to reduce the problem on the periodic grating to the unit cell with quasi periodic boundary conditions [14, 6, 17]. One crucial task is to treat the infinite domains above and below the grating. Commonly used possibilities are the perfectly matched layers (PML) technique [3, 28], or transparent boundary conditions [1, 2, 4, 13, 31], derived by integral equation methods. The second method can be efficiently implemented on uniform grids by the fast Fourier transform. Our new approach is based on the method of Nitsche [24, 34, 11] and works with a priori independent approximation spaces for the near and the far-field. Continuity is obtained by the variational formulation. This allows us to work with finite elements in the complicated grating region, while propagating and evanescent waves are best suited for describing the far-field. Substrate layers modeled with the transfer-matrix-method [23, 27] fit well into this concept. The implementation requires the evaluation of integrals of products of the different basis functions, which is done by standard numerical integration rules. In order to achieve high accuracy, high order Nédélec elements [21, 20, 33, 36, 12] are used.
The paper is organized as follows: In Section 2 the diffraction problem is described to the reader, and a plane wave expansion (Rayleigh expansion) is stated for the far-field region. In Section 3 the variational formulation is derived for the near field region, and quasi periodic boundary conditions are incorporated in order to reduce the problem onto a unit cell. The coupling between these two regions with Nitsche's method concludes this section. Section 4 studies the modeling of substrate layers and the paper finishes with some numerical experiments in the last section.

2 Preliminaries

First we start with some definitions. The domain $\Omega^I := \{(x, y, z) : a < z < b\}$ for $a < b$ represents the interior domain, the exterior domains are defined according to Figure 1 as $\Omega^+ := \{(x, y, z) : z > b\}$ and $\Omega^- = \{(x, y, z) : z < a\}$ and we set $\Omega^\pm := \Omega^+ \cup \Omega^-$. In order to calculate the diffraction and transmission pattern of gratings, we consider a structure in $\mathbb{R}^3$, which is periodic in x and y direction with periodes d_x and d_y. By using this periodicity, material parameters like the electric permittivity ε and the magnetic permeability μ are invariant under translation in

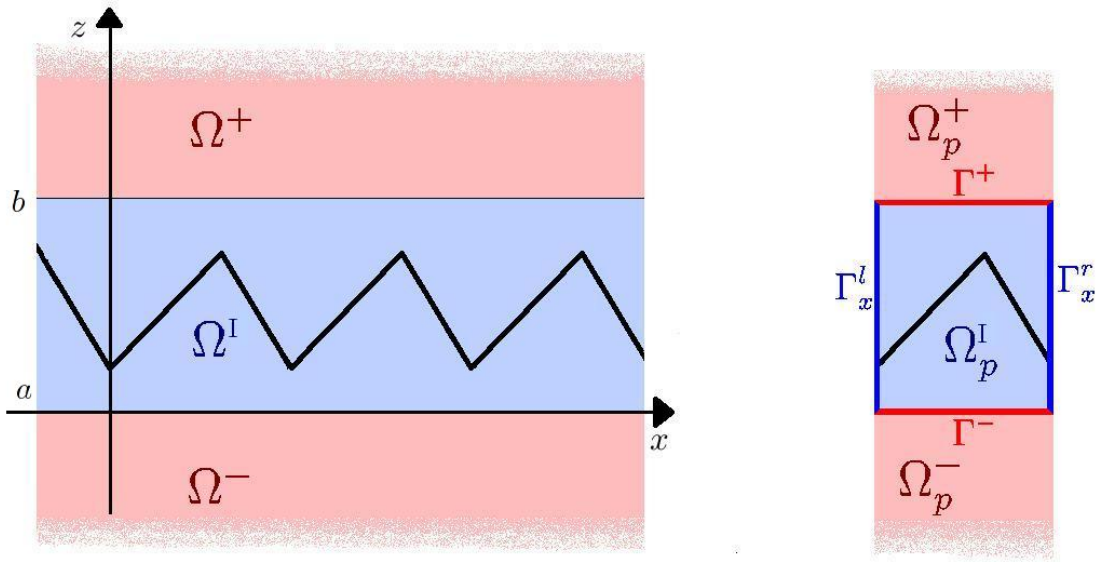

Figure 1: geometry of the problem

x and y direction

$$\varepsilon(x + nd_x, y + md_y, z) = \varepsilon(x, y, z),$$
$$\mu(x + nd_x, y + md_y, z) = \mu(x, y, z)$$

with $n, m \in \mathbb{Z}$. In the domain Ω^I $\varepsilon(\mathbf{x})$ and $\mu(\mathbf{x})$ are piecewise constant functions. The permeability μ is assumed to be real and positive and ε is a complex-valued function. Introducing a complex permittivity, we are able to describe absorption (and emission) by the material. In the far-field region, which is represented by the domains Ω^+ and Ω^-, the functions $\varepsilon(\mathbf{x})$ and $\mu(\mathbf{x})$ are constant with values ε^+, μ^+ and ε^-, μ^- respectively. The material in the domain Ω^+ is assumed to be absorption free with a real valued ε^+.

2.1 Maxwell's equations

If there are no current-sources and no free charges in the grating, the electromagnetic fields for all points $\mathbf{x} \in \mathbb{R}^3$ can be described by the time-harmonic Maxwell's

equations

$$\nabla \times \mathbf{E}(\mathbf{x}) = i\omega\mu(\mathbf{x})\mathbf{H}(\mathbf{x}), \quad (1)$$
$$\nabla \times \mathbf{H}(\mathbf{x}) = -i\omega\varepsilon(\mathbf{x})\mathbf{E}(\mathbf{x}), \quad (2)$$

where $\mathbf{E}(\mathbf{x})$ and $\mathbf{H}(\mathbf{x})$ denote the electric and magnetic field vectors, and ω represents the angular frequency. Eliminating the magnetic field, we end up with the second order equation

$$\nabla \times \left[\frac{1}{\mu}\nabla \times \mathbf{E}\right] = \omega^2\varepsilon\mathbf{E}. \quad (3)$$

2.2 Rayleigh expansion for the far-field

In the following discussion an arbitrary coefficient, which has the value a^+ in Ω^+ and a^- in Ω^- is denoted as $a^\pm$. In the domains Ω^+ and Ω^- where $\varepsilon(\mathbf{x})$ and $\mu(\mathbf{x})$ are constant scalar functions, equation (3) reduces to

$$\nabla \times (\nabla \times \mathbf{E}) = \left(k^\pm\right)^2 \mathbf{E} \qquad \text{in } \Omega^\pm,$$

The coefficient $(k^\pm)^2 := \omega^2 (\nu^\pm)^2$ is the absolute value of the wavevector including the refractive index $\nu^\pm := \sqrt{\epsilon^\pm \mu^\pm}$ with a non negative imaginary part $\mathrm{Im}(\nu^\pm) \geq 0$ and for $\mathrm{Im}(\nu^\pm) = 0$ the real part has to be positive $\mathrm{Re}(\nu^\pm) > 0$. Fundamental solutions of this equation are plane waves

$$\mathbf{E}(\mathbf{x}) = \mathbf{A}e^{i(\alpha x+\beta y+\gamma z)}$$

satisfying the constraint

$$\alpha^2 + \beta^2 + \gamma^2 = k^2 \quad \text{with} \quad \alpha, \beta, \gamma \in \mathbb{C}.$$

The parameters α, β and γ describe the components of the wavevector $\mathbf{k}$ which indicates the direction of propagation of the plane wave, and $\mathbf{A}$ is a constant vector representing the amplitude. By taking the divergence of equation (2), it follows immediately that $\varepsilon\mathbf{E}$ is divergence free. Consequently the vector-product $\mathbf{k}\cdot\mathbf{A}$ has to be zero and the electric field vector is orthogonal to the wavevector.
The electric field of the incident light can be expressed as a plane wave with the wavevector

$$\mathbf{k}_{00}^+ = (\alpha_0^+, \beta_0^+, \gamma_{00}^+) = k^+ (\cos\theta\cos\phi, \cos\theta\sin\phi, -\sin\theta). \quad (4)$$

Here $\theta \in [0, \frac{\pi}{2})$ and $\phi \in [0, 2\pi)$ are the angles of incidence. Combining this with the theory of Bloch Floquet [14, 6, 17]

$$\mathbf{E}(\mathbf{x} + d_x\mathbf{e}_x) = \rho_x\mathbf{E}(\mathbf{x}), \quad (5)$$
$$\mathbf{E}(\mathbf{x} + d_y\mathbf{e}_y) = \rho_y\mathbf{E}(\mathbf{x}), \quad (6)$$

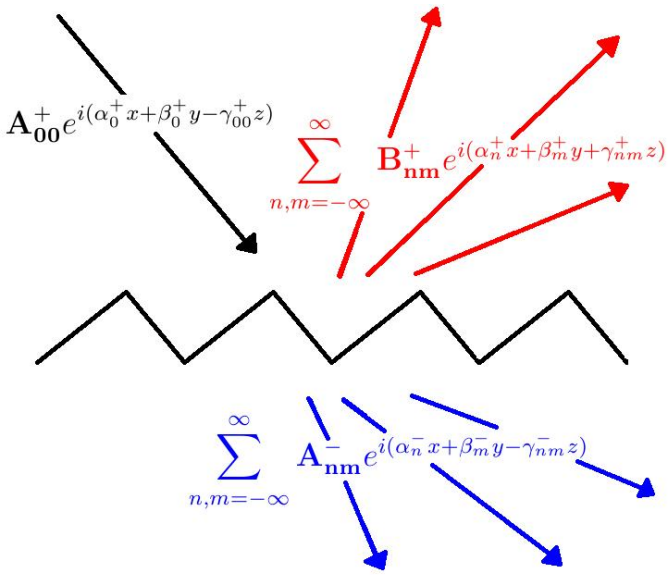

Figure 2: the Rayleigh expansion

with the unit vectors in x- and y-direction $\mathbf{e}_x$ and $\mathbf{e}_y$, and ρ_x, ρ_y given by the incoming wave, we get a further restriction for the wavevectors of our plane waves

$$\alpha_n^{\pm} = \alpha_0^+ + n\frac{2\pi}{d_x}, \tag{7}$$

$$\beta_m^{\pm} = \beta_0^+ + m\frac{2\pi}{d_y}, \tag{8}$$

$$\gamma_{nm}^{\pm} = \sqrt{(k^{\pm})^2 - (\alpha_n^{\pm})^2 - (\beta_m^{\pm})^2}, \tag{9}$$

where $n, m \in \mathbb{Z}$. For non-absorbing materials, the variables $\alpha_n^{\pm}$ and $\beta_m^{\pm}$ are supposed to be real, but $\gamma_{nm}^{\pm}$ can be complex. The squareroot is defined such that for the real part of $\gamma_{nm}^{\pm}$ $\mathrm{Re}(\gamma_{nm}^{\pm}) \geq 0$ is valid. If the imaginary part of $\gamma_{nm}^{\pm}$ is different from zero the wave is evanescent and damped in $z-$direction.

Collecting this, we obtain the Rayleigh expansion of the field in the exterior domains $\Omega^{\pm}$

$$\mathbf{E}(\mathbf{x}) = \sum_{n,m=-\infty}^{\infty} \mathbf{A}_{nm}^{\pm} e^{i(\alpha_n^{\pm} x+\beta_m^{\pm} y-\gamma_{nm}^{\pm} z)} + \sum_{n,m=-\infty}^{\infty} \mathbf{B}_{nm}^{\pm} e^{i(\alpha_n^{\pm} x+\beta_m^{\pm} y+\gamma_{nm}^{\pm} z)}. \tag{10}$$

The plane waves of the first sum are propagating into negative $z-$direction and those of the second one into positive $z-$direction. As plotted in Figure 2 we

assume that only the incident wave is propagating from above towards the grating. Consequently all $\mathbf{A}^+_{\mathbf{nm}}$ except for $m = n = 0$ are zero. In the domain Ω^- no incident wave from below is expected, thus all $\mathbf{B}^-_{\mathbf{nm}}$ are zero. Hence the field in the exterior domains is defined as

$$\mathbf{E}(\mathbf{x}) = \begin{cases} \mathbf{E}_{in}(\mathbf{x}) + \mathbf{E}^+(\mathbf{x}) & \text{in } \Omega^+ \\ \mathbf{E}^-(\mathbf{x}) & \text{in } \Omega^- \end{cases} \tag{11}$$

with

$$\mathbf{E}_{in}(\mathbf{x}) = \mathbf{A}^+_{00} e^{i(\alpha^+_0 x + \beta^+_0 y - \gamma^+_{00} z)}, \tag{12}$$

$$\mathbf{E}^+(\mathbf{x}) = \sum_{n,m=-\infty}^{\infty} \mathbf{B}^+_{nm} e^{i(\alpha^+_n x + \beta^+_m y + \gamma^+_{nm} z)}, \tag{13}$$

$$\mathbf{E}^-(\mathbf{x}) = \sum_{n,m=-\infty}^{\infty} \mathbf{A}^-_{nm} e^{i(\alpha^-_n x + \beta^-_m y - \gamma^-_{nm} z)}. \tag{14}$$

2.3 Reflection and transmission coefficients

The Rayleigh coefficients of the reflected and transmitted plane waves are closely related to the reflection and transmission coefficients $\mathcal{R}$ and $\mathcal{T}$ of this waves. These coefficients can be interpreted as the fraction of energy transported by such a diffracted mode and the incident energy. In the following discussion complex conjugation of a quantity a is denoted as $\overline{a}$.
For an arbitrary electric field $\mathbf{E}(\mathbf{x})$ with harmonic time dependence and the corresponding magnetic field $\mathbf{H}(\mathbf{x})$ the time average of the Poynting vector $\mathbf{S}(\mathbf{x})$, which specifies the energy flow (or more precisely the density of this flow), is defined as [7, 16]

$$\mathbf{S}(\mathbf{x}) = \frac{c}{8\pi} \mathrm{Re}\left(\mathbf{E}(\mathbf{x}) \times \overline{\mathbf{H}}(\mathbf{x})\right),$$

where c denotes the speed of light. Assuming that the electric field is a plane wave i.e. $\mathbf{E}(\mathbf{x}) = \mathbf{E}_R\, e^{i\mathbf{k}\cdot\mathbf{x}}$, we end up with a constant Poynting vector

$$\mathbf{S} = \frac{c}{8\pi} |\mathbf{E}_R|^2 \mathrm{Re}\left(\frac{1}{\omega\mu}\overline{\mathbf{k}}\right).$$

Knowing the Poynting vector we are now able to calculate the reflection or transmission coefficient of the grating for a certain diffracted mode. In doing so, we have to divide the energy of the reflected wave going through an area $A(x, y)$ parallel to the plane of the grating (the $x - y$ plane) by the energy of the incident wave going through the same area. The energy flow $\mathcal{E}$ through this area is defined as

$$\mathcal{E} = \int_{A(x,y)} \mathbf{S} \cdot \mathbf{e}_z \, dA,$$

the vector $(0,0,1)^T$ denoted by $\mathbf{e}_z$. The reflection coefficient $\mathcal{R}_{nm}$ and the transmission coefficient $\mathcal{T}_{nm}$ respectively for any order of diffraction n, m can then be obtained via

$$\mathcal{R}_{nm} = \frac{|\mathbf{B}^+_{nm}|^2 \operatorname{Re}(\overline{\gamma}^+_{nm})}{|\mathbf{A}^+_{00}|^2 \operatorname{Re}(\overline{\gamma}^+_{00})}, \qquad \mathcal{T}_{nm} = \frac{|\mathbf{A}^-_{nm}|^2 \, \mu^+ \operatorname{Re}(\overline{\gamma}^-_{nm})}{|\mathbf{A}^+_{00}|^2 \, \mu^- \operatorname{Re}(\overline{\gamma}^+_{00})}.$$

3 Problem formulations and discretization

In the previous section we stated a plane wave ansatz for the solution of equation (3) in the domains Ω^+ and Ω^- including the unknown coefficients $\mathbf{A}^-_{nm}$ and $\mathbf{B}^+_{nm}$. By solving equation (3) in the interior domain Ω^I with finite elements and by coupling the solution to the plane waves of the domains Ω^+ and Ω^-, these coefficients can be calculated.
Since we have a periodic structure, we restrict the infinite domain Ω^I to the unit-cell Ω^I_p of the grating (compare Figure 1). We denote the restrictions of Ω^+ and Ω^- as Ω^+_p and Ω^-_p. Γ^+ and Γ^- represent the interfaces between these domains, and they are defined as $\Gamma^+ := \overline{\Omega}^I_p \cup \overline{\Omega}^+_p$ and $\Gamma^- := \overline{\Omega}^I_p \cup \overline{\Omega}^-_p$. The two periodic boundaries perpendicular to the $x-$axis are called Γ^l_x and Γ^r_x, whereas Γ^l_y and Γ^r_y describe the boundaries orthogonal to the $y-$axis.

3.1 Classical formulation of the problem

According to the theory of Bloch-Floquet [14, 6, 17] the solution in the domain Ω^I_p in a periodic structure is quasi-periodic and the equations (5) and (6) are valid. As the incident plane wave has to fullfill this quasi-periodicity, we are able to specify the corresponding factors $\rho_x = e^{-i\alpha^+_0 d_x}$ for x-direction and $\rho_y = e^{-i\beta^+_0 d_y}$ for y-direction. This leads us to the formulation of the quasi periodic boundary conditions for the tangential component of the electric and magnetic field

$$\mathbf{n} \times \mathbf{E}^I(\mathbf{x}) = \rho_x \mathbf{n} \times \mathbf{E}^I(\mathbf{x} + \mathbf{e}_x d_x) \qquad \forall \mathbf{x} \in \Gamma^l_x, \tag{15}$$

$$\mathbf{n} \times \frac{1}{\mu}\left(\nabla \times \mathbf{E}^I(\mathbf{x})\right) = \rho_x \mathbf{n} \times \frac{1}{\mu}\left(\nabla \times \mathbf{E}^I(\mathbf{x} + \mathbf{e}_x d_x)\right) \qquad \forall \mathbf{x} \in \Gamma^l_x, \tag{16}$$

$$\mathbf{n} \times \mathbf{E}^I(\mathbf{x}) = \rho_y \mathbf{n} \times \mathbf{E}^I(\mathbf{x} + \mathbf{e}_y d_y) \qquad \forall \mathbf{x} \in \Gamma^l_y, \tag{17}$$

$$\mathbf{n} \times \frac{1}{\mu}\left(\nabla \times \mathbf{E}^I(\mathbf{x})\right) = \rho_y \mathbf{n} \times \frac{1}{\mu}\left(\nabla \times \mathbf{E}^I(\mathbf{x} + \mathbf{e}_y d_y)\right) \qquad \forall \mathbf{x} \in \Gamma^l_y \tag{18}$$

with the outer-normal-vector to the surface Γ^l_x and Γ^l_y, respectively, denoted as $\mathbf{n}$. On the boundaries Γ^+ and Γ^- the finite element solution of the domain Ω^I_p has to match the plane wave solutions of the domains Ω^+_p and Ω^-_p. On these interfaces

the tangential component of the magnetic and electric fields have to be continuous, which are the interface conditions

$$\mathbf{n} \times \mathbf{E}^I(\mathbf{x}) = \mathbf{n} \times (\mathbf{E}_{in}(\mathbf{x}) + \mathbf{E}^+(\mathbf{x})) \qquad \forall \mathbf{x} \in \Gamma^+, \quad (19)$$

$$\mathbf{n} \times \frac{1}{\mu} \left(\nabla \times \mathbf{E}^I(\mathbf{x})\right) = \mathbf{n} \times \frac{1}{\mu} \left(\nabla \times (\mathbf{E}_{in}(\mathbf{x}) + \mathbf{E}^+(\mathbf{x}))\right) \qquad \forall \mathbf{x} \in \Gamma^+, \quad (20)$$

$$\mathbf{n} \times \mathbf{E}^I(\mathbf{x}) = \mathbf{n} \times \mathbf{E}^-(\mathbf{x}) \qquad \forall \mathbf{x} \in \Gamma^-, \quad (21)$$

$$\mathbf{n} \times \frac{1}{\mu} \left(\nabla \times \mathbf{E}^I(\mathbf{x})\right) = \mathbf{n} \times \frac{1}{\mu} \left(\nabla \times \mathbf{E}^-(\mathbf{x})\right) \qquad \forall \mathbf{x} \in \Gamma^-, \quad (22)$$

with the electric fields $\mathbf{E}^+$ and $\mathbf{E}^-$ obtained by (10) and the outer-normal-vector $\mathbf{n}$.
Summarizing this we end up with the formulation of the classical problem in the domain Ω_p^I:

Problem 1. *[classical formulation] Find a vector-valued function* $\mathbf{E}(\mathbf{x})$ *which satisfies*

$$\nabla \times \frac{1}{\mu(\mathbf{x})}(\nabla \times \mathbf{E}^I(\mathbf{x})) = \omega^2 \varepsilon(\mathbf{x}) \mathbf{E}^I(\mathbf{x}) \qquad \text{in } \Omega_p^I. \quad (23)$$

under the quasi-periodic boundary conditions (15)-(18), the interface conditions (19)-(22) and the ansatz (11)-(14) on $\Omega^{\pm}$.

3.2 The weak formulation

Now we are able to state the variational formulation for the described problem in the domain Ω_p^I. Starting with equation (23), multiplying it with a testfunction, integrating it over the whole domain Ω_p^I and integrating by parts, we end up with the variational equation

$$\int_{\Omega_p^I} \frac{1}{\mu} \left(\nabla \times \mathbf{E}^I\right) \cdot (\nabla \times \overline{\mathbf{v}}) \; d\mathbf{x} + \int_{\partial\Omega_p^I} \left[\mathbf{n} \times \frac{1}{\mu} \left(\nabla \times \mathbf{E}^I\right)\right] \cdot \overline{\mathbf{v}} \; d\mathbf{x} - \int_{\Omega_p^I} \omega^2 \varepsilon \mathbf{E}^I \cdot \overline{\mathbf{v}} \; d\mathbf{x} = 0 \quad (24)$$

for $\mathbf{E}^I(\mathbf{x}) \in H(\text{curl}, \Omega_p^I) = \left\{\mathbf{v} \in (L_2(\Omega_p^I))^3 \; : \; \text{curl } \mathbf{v} \in (L_2(\Omega_p^I))^3\right\}$ and all $\mathbf{v}(\mathbf{x}) \in H(\text{curl}, \Omega_p^I)$.
Here we have still to keep the quasi-periodic boundary conditions (15)-(18) and the interface conditions (19)-(22) in mind.

3.3 Incorporation of quasi-periodic boundary conditions

The next step is to incorporate the quasi-periodic boundary conditions (15)-(18). First we define the periodic space

$$V_p^I := \{\mathbf{v} \in H(\mathrm{curl}, \Omega_p^I) \ : \mathbf{n} \times \mathbf{v}(\mathbf{x}) = \rho_x \mathbf{n} \times \mathbf{v}(\mathbf{x} + \mathbf{e_x} d_x) \ \forall \mathbf{x} \in \Gamma_x^l, \\ \mathbf{n} \times \mathbf{v}(\mathbf{x}) = \rho_y \mathbf{n} \times \mathbf{v}(\mathbf{x} + \mathbf{e_y} d_y) \ \forall \mathbf{x} \in \Gamma_y^l\} \tag{25}$$

with the outer-normal-vector $\mathbf{n}$ to Γ_x^l and Γ_y^l. The periodic constraints (15) and (17) are essential ones and they are incorporated directly into the testspace. The conditions (16) and (18) are natural and they are included in weak sense.

Lemma 1. *Any function $\mathbf{E}^I \in V_p^I$ satisfying the variational equation*

$$\int_{\Omega_p^I} \frac{1}{\mu} \left(\nabla \times \mathbf{E}^I\right) \cdot (\nabla \times \overline{\mathbf{v}}) \ d\mathbf{x} + \int_{\Gamma^\pm} \left[\mathbf{n} \times \frac{1}{\mu} \left(\nabla \times \mathbf{E}^I\right)\right] \cdot \overline{\mathbf{v}} \ d\mathbf{x} - \int_{\Omega_p^I} \omega^2 \varepsilon \mathbf{E}^I \cdot \overline{\mathbf{v}} \ d\mathbf{x} = 0 \tag{26}$$

for all $\mathbf{v} \in V_p^I$ fullfills the differential equation (23) together with the quasi-periodic boundary conditions (15)-(18).

Proof. The conditions (15) and (17) are fullfilled by the definition of V_p^I.
Integration by parts yields

$$\int_{\Omega_p^I} \left(\nabla \times \frac{1}{\mu}(\nabla \times \mathbf{E}^I) - \omega^2 \varepsilon \mathbf{E}^I\right) \cdot \overline{\mathbf{v}} \ d\mathbf{x} - \int_{\Gamma_x^l \cup \Gamma_x^r} \left(\mathbf{n} \times \frac{1}{\mu}(\nabla \times \mathbf{E}^I)\right) \cdot \overline{\mathbf{v}} \ d\mathbf{x} \\ - \int_{\Gamma_y^l \cup \Gamma_y^r} \left(\mathbf{n} \times \frac{1}{\mu}(\nabla \times \mathbf{E}^I)\right) \cdot \overline{\mathbf{v}} \ d\mathbf{x} = 0.$$

By choosing $\mathbf{v}$ such that $\mathbf{n} \times \mathbf{v}|_{\Gamma_p} = 0$ with $\Gamma_p = \Gamma_x^l \cup \Gamma_x^r \cup \Gamma_y^l \cup \Gamma_y^r$ we obtain

$$\nabla \times \frac{1}{\mu} \left(\nabla \times \mathbf{E}^I\right) - \omega^2 \varepsilon \mathbf{E}^I = 0 \tag{27}$$

Next we choose $\mathbf{v}$ such that $\mathbf{n} \times \mathbf{v}|_{\Gamma_y^l \cup \Gamma_y^r} = 0$. Exchanging the outer-normal-vector on Γ_x^r in the corresponding integral by the negative outer-normal-vector on Γ_x^l and using $\rho_x \mathbf{n} \times \overline{\mathbf{v}}(\mathbf{x}) = \mathbf{n} \times \overline{\mathbf{v}}(\mathbf{x} + d_x \mathbf{e}_x)$ from the definition of the space, we observe

$$0 = -\int_{\Gamma_x^l} \frac{1}{\mu} \left(\nabla \times \mathbf{E}^I(\mathbf{x})\right) \cdot (\overline{\mathbf{v}}(\mathbf{x}) \times \mathbf{n}) \ d\mathbf{x} \\ + \int_{\Gamma_x^l} \rho_x \frac{1}{\mu} \left(\nabla \times \mathbf{E}^I(\mathbf{x} + d_x \mathbf{e}_x)\right) \cdot (\overline{\mathbf{v}}(\mathbf{x}) \times \mathbf{n}) \ d\mathbf{x}$$

$$0 = -\int_{\Gamma_x^l} \left(\mathbf{n} \times \frac{1}{\mu}(\nabla \times \mathbf{E}^I(\mathbf{x})) - \mathbf{n} \times \frac{1}{\mu}(\nabla \times \mathbf{E}^I(\mathbf{x} + d_x \mathbf{e}_x))\right) \cdot \overline{\mathbf{v}}(\mathbf{x}) \ d\mathbf{x} = 0.$$

This results in condition (16). Choosing a testfunction $\mathbf{v}$ such that $\mathbf{n} \times \mathbf{v}|_{\Gamma_x^l \cup \Gamma_x^r} = 0$ we obtain condition (18). □

3.4 Incorporation of the interface conditions by Nitsche's Method

The final step is the incorporation of the interface conditions into our variational formulation (26). The polynomial solution in the domain Ω_p^I has to be coupled across the interfaces Γ^+ and Γ^- to the plane wave solution (10), and we have to fullfill the interface conditions (19)-(22). Furthermore the given incident plane wave is incorporated. First we introduce some notations:
The wavevectors $\mathbf{k}_{nm}^+ := (\alpha_n^+, \beta_m^+, \gamma_{nm}^+)$ and $\mathbf{k}_{nm}^- := (\alpha_n^-, \beta_m^-, -\gamma_{nm}^-)$ are defined according to the equations (7)-(9), and $\mathbf{k}_0^+$ denotes the wavevector of the incoming wave from equation (4). Using this we are able to introduce the plane wave spaces

$$V^+ = \Big\{\mathbf{v} : \mathbf{v} = \sum_{n=-\infty}^{\infty}\sum_{m=-\infty}^{\infty} \mathbf{B}_{nm}^+ e^{i\mathbf{k}_{nm}^+\cdot\mathbf{x}}, \quad \mathbf{B}_{nm}^+ \in \mathbb{R}^3, \quad \mathbf{B}_{nm}^+ \cdot \mathbf{k}_{nm}^+ = 0\Big\},$$

$$V^- = \Big\{\mathbf{v} : \mathbf{v} = \sum_{n=-\infty}^{\infty}\sum_{m=-\infty}^{\infty} \mathbf{A}_{nm}^- e^{i\mathbf{k}_{nm}^-\cdot\mathbf{x}}, \quad \mathbf{A}_{nm}^- \in \mathbb{R}^3, \quad \mathbf{A}_{nm}^- \cdot \mathbf{k}_{nm}^- = 0\Big\}$$

on the domains Ω^+ and Ω^-, respectively. We define the scalar products

$$\Big(\mathbf{u}, \mathbf{v}\Big)_{\Omega_p^I} := \int_{\Omega_p^I} \mathbf{u} \cdot \overline{\mathbf{v}}\, d\mathbf{x} \qquad \text{and} \qquad \Big\langle \mathbf{u}, \mathbf{v} \Big\rangle_{\Gamma^\pm} := \int_{\Gamma^+\cup\Gamma^-} \mathbf{u} \cdot \overline{\mathbf{v}}\, d\mathbf{x}.$$

Keeping the incoming plane wave in mind, the incorporation of the interfaceconditions (19)-(22) with Nitsche's method [24, 34, 11] yields the following problemformulation:

Problem 2. *Find* $\big(\mathbf{E}^I, \mathbf{E}^\pm\big) = u \in V = V_p^I \times V^\pm = V_p^I \times V^+ \times V^-$ *such that*

$$a(u, v) = f(v) \qquad \forall v = (\mathbf{v}^I, \mathbf{v}^\pm) \in V \tag{28}$$

with the bilinear-form

$$\begin{aligned} a(u,v) =& \Big(\mu^{-1}(\nabla \times \mathbf{E}^I), \nabla \times \mathbf{v}^I\Big)_{\Omega_p^I} - \Big(\omega^2 \varepsilon \mathbf{E}^I, \mathbf{v}^I\Big)_{\Omega_p^I} \\ &- \Big\langle \mu^{-1}(\nabla \times \mathbf{E}^\pm), (\mathbf{n} \times \mathbf{v}^I - \mathbf{n} \times \mathbf{v}^\pm)\Big\rangle_{\Gamma^\pm} - \Big\langle \mu^{-1}(\nabla \times \mathbf{E}^\pm), \mathbf{n} \times \mathbf{v}^\pm\Big\rangle_{\Gamma^\pm} \\ &- \Big\langle (\mathbf{n} \times \mathbf{E}^I - \mathbf{n} \times \mathbf{E}^\pm), \mu^{-1}(\nabla \times \mathbf{v}^\pm)\Big\rangle_{\Gamma^\pm} \\ &+ \eta\Big\langle (\mathbf{n} \times \mathbf{E}^I - \mathbf{n} \times \mathbf{E}^\pm), (\mathbf{n} \times \mathbf{v}^I - \mathbf{n} \times \mathbf{v}^\pm)\Big\rangle_{\Gamma^\pm} \end{aligned} \tag{29}$$

where we assume the stabilizing parameter η to be sufficiently large. The linear-form contains the incident wave $\mathbf{E}_{in} := \mathbf{A}^+_{00} e^{i\mathbf{k}_0^+ \cdot \mathbf{x}}$ as

$$\begin{aligned} f(v) \ &= \Big\langle \mu^{-1}(\nabla \times \mathbf{E}_{in}), \mathbf{n} \times \mathbf{v}^I \Big\rangle_{\Gamma^\pm} - \Big\langle \mathbf{n} \times \mathbf{E}_{in}, \mu^{-1}(\nabla \times \mathbf{v}^+) \Big\rangle_{\Gamma^\pm} \\ &\quad + \eta \Big\langle \mathbf{n} \times \mathbf{E}_{in}(\mathbf{n} \times \mathbf{v}^I - \mathbf{n} \times \mathbf{v}^+) \Big\rangle_{\Gamma^\pm}. \end{aligned}$$

The following Lemma states consistency of this Problem and the classical formulation in Problem 1 with its exact solution $\mathbf{E}^I$ and $\mathbf{E}^\pm$according to definition (11).

Lemma 2. *The exact solution $u = (\mathbf{E}^I,\ \mathbf{E}^+,\ \mathbf{E}^-)$ solves the discrete variational problem*

$$a(u, v) = f(v) \qquad \forall v \in V.$$

Proof. Inserting $u = (\mathbf{E}^I, \mathbf{E}^+ + \mathbf{E}_{in} - \mathbf{E}_{in},\ \mathbf{E}^-)$ into $a(u, v) - f(v)$, and knowing from the interface condition (19) and (21) that $\mathbf{n} \times \mathbf{E}^I - (\mathbf{n} \times \mathbf{E}^+ + \mathbf{E}_{in}) = 0$ on Γ^+ and $\mathbf{n} \times \mathbf{E}^I - \mathbf{n} \times \mathbf{E}^- = 0$ on Γ^-, we arrive at:

$$\begin{aligned} a(w, v) - f(v) &= \Big(\mu^{-1}(\nabla \times \mathbf{E}^I), \nabla \times \mathbf{v}^I\Big)_{\Omega_p^I} - \Big(\omega^2 \varepsilon \mathbf{E}^I, \mathbf{v}^I\Big)_{\Omega_p^I} \\ &\quad - \Big\langle \mu^{-1}(\nabla \times (\mathbf{E}^+ + \mathbf{E}_{in})), (\mathbf{n} \times \mathbf{v}^I - \mathbf{n} \times \mathbf{v}^\pm) \Big\rangle_{\Gamma^+} - \Big\langle \mu^{-1}(\nabla \times (\mathbf{E}^+ + \mathbf{E}_{in})), \mathbf{n} \times \mathbf{v}^\pm \Big\rangle_{\Gamma^+} \\ &\quad - \Big\langle \mu^{-1}(\nabla \times \mathbf{E}^-), (\mathbf{n} \times \mathbf{v}^I - \mathbf{n} \times \mathbf{v}^\pm) \Big\rangle_{\Gamma^-} - \Big\langle \mu^{-1}(\nabla \times \mathbf{E}^-), \mathbf{n} \times \mathbf{v}^\pm \Big\rangle_{\Gamma^-} \\ a(w, v) - f(v) &= \Big(\mu^{-1}(\nabla \times \mathbf{E}^I), \nabla \times \mathbf{v}^I\Big)_{\Omega_p^I} - \Big(\omega^2 \varepsilon \mathbf{E}^I, \mathbf{v}^I\Big)_{\Omega_p^I} \\ &\quad - \Big\langle \mu^{-1}(\nabla \times (\mathbf{E}^+ + \mathbf{E}_{in})), \mathbf{n} \times \mathbf{v}^I \Big\rangle_{\Gamma^+} - \Big\langle \mu^{-1}(\nabla \times \mathbf{E}^-), \mathbf{n} \times \mathbf{v}^I \Big\rangle_{\Gamma^-}. \end{aligned}$$

With the help of condition (20) and (22) we can replace $\mathbf{n} \times \mu^{-1}(\nabla \times (\mathbf{E}^+ + \mathbf{E}_{in}))$ by $\mathbf{n} \times \mu^{-1}(\nabla \times \mathbf{E}^I)$ and $\mathbf{n} \times \mu^{-1}(\nabla \times \mathbf{E}^-)$ by $\mathbf{n} \times \mu^{-1}(\nabla \times \mathbf{E}^I)$, and we obtain

$$\begin{aligned} a(w, v) - f(v) &= \Big(\mu^{-1}(\nabla \times \mathbf{E}^I), \nabla \times \mathbf{v}^I\Big)_{\Omega_p^I} - \Big(\omega^2 \varepsilon \mathbf{E}^I, \mathbf{v}^I\Big)_{\Omega_p^I} \\ &\quad + \Big\langle \mathbf{n} \times \mu^{-1}(\nabla \times \mathbf{E}^I), \mathbf{v}^I \Big\rangle_{\Gamma^\pm}. \end{aligned}$$

By Lemma 1 we know, that this expression is zero. □

Remarks:

- Using this method, the Rayleigh coefficients of the reflected ($\mathbf{B}^+_{nm}$) and transmitted waves ($\mathbf{A}^-_{nm}$) appear as additional unknowns in the variational equation (28).

- The incident plane wave $\mathbf{A}_{00}^{+}e^{i\mathbf{k}_0^{+}\cdot\mathbf{x}}$ is incorporated directly into the testspace by homogenizing the problem.

- During the assembling of the stiffnessmatrix we can evaluate the curl of a plane wave instead of the curl of polynomial basis functions, i.e. $\nabla\times\mathbf{E}^{\pm}$ instead of $\nabla\times\mathbf{E}^{I}$ in the domain Ω_p^I, which is cheaper. The curl of a plane wave is proportional to the cross product of wavevector and plane wave. Evaluating the curl is then equivalent to the evaluation of the basisfunction.

- The bilinearform (29) shows that the stiffnessmatrix, except to the contribution of the integral $\left\langle \mu^{-1}(\nabla\times\mathbf{E}^{\pm}),\mathbf{n}\times\mathbf{v}^{\pm}\right\rangle_{\Gamma^{\pm}}$, is hermitian. Here, the product of two plane waves is integrated over the interface. Because of

$$\int_0^d e^{i(k_0+n\frac{2\pi}{d})x}e^{-i(k_0+m\frac{2\pi}{d})x}dx=\delta_{nm}d$$

  with the Kronecker Delta δ_{nm}, there is only a contribution of this non hermitian term to the diagonal of the stiffness matrix. Hence the stiffnessmatrix can be decomposed into an hermitian and a diagonal matrix.

4 The modeling of substrate layers

In practical applications there are often layers between the grating and the semi-infinite substrate. One possibility to take them into account is to include these layers into the Finite Element Domain Ω_p^I, which may result in a large number of unknowns. An alternative would be to include these layers into the boundary conditions. In this case we have to allow for waves which are reflected by the layers, and consequently incident waves from below the grating are present. The aim of this section is to express the Rayleigh coefficients of the waves leaving the layers and propagating towards the grating (B_F in Figure 3) in terms of the coefficients of the waves leaving the grating and propagating towards the stack (A_F in Figure 3) via the transfer matrix method [23, 27]. Doing this we are able to incorporate the substrate layers directly into the function space.

In the following discussion the layers are assumed to be parallel to the $x-y$ plane. The permittivity ε jumps on the layer interfaces while μ is assumed to be constant in the whole stack. Because the material parameters are constant in every layer, the field there can be written as a sum of plane waves. Knowing that diffraction of a plane wave at a plane surface results in one reflected and one transmitted wave, the sum of plane waves in every layer reduces to an up going and a down going wave, if there is only one wave incidenting onto a stack of layers.

Since the polarization of the electromagnetic field is not changed by a plane surface

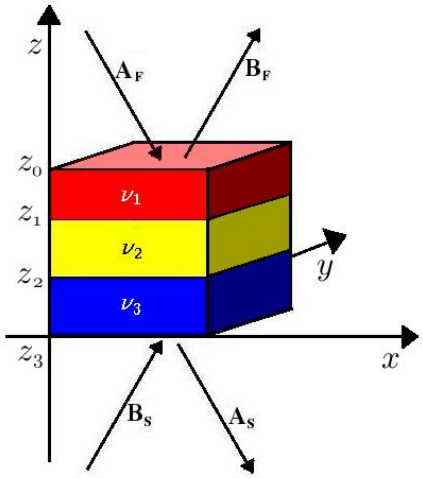

Figure 3: a stack of substrate layers

for TE and TM polarized light, it is convenient to split the incident field into a TE and a TM contribution. In the TE-case the electric field is parallel to the surface of the layer, while the magnetic field is perpendicular to the wavevector and the electric field. In the TM-case the situation is vice versa.

4.1 TE-modes

First we consider the $j-$th layer of the stack between $z = z_j$ and $z = z_{j-1}$ (compare Figure 3) with thickness $\delta_j = z_{j-1} - z_j$. For TE-modes the electric field $E_\parallel$ is parallel to layers and it can be decomposed as

$$E_\parallel(x, y, z) = A_j e^{i(\alpha_j x + \beta_j y - \gamma_j z)} + B_j e^{i(\alpha_j x + \beta_j y + \gamma_j z)}.$$

Using this representation we can describe the electric field and its normal flux at the boundaries below and on top of the layer

$$\begin{aligned} \begin{pmatrix} E_\parallel \\ \frac{\partial E_\parallel}{\partial z} \end{pmatrix}\Big|_{z=z_j} &= \begin{pmatrix} 1 & 1 \\ -i\gamma_j & i\gamma_j \end{pmatrix} \begin{pmatrix} A_j e^{i(\alpha_j x + \beta_j y - \gamma_j z_j)} \\ B_j e^{i(\alpha_j x + \beta_j y + \gamma_j z_j)} \end{pmatrix}, \\ \begin{pmatrix} E_\parallel \\ \frac{\partial E_\parallel}{\partial z} \end{pmatrix}\Big|_{z=z_{j-1}} &= \begin{pmatrix} 1 & 1 \\ -i\gamma_j & i\gamma_j \end{pmatrix} \begin{pmatrix} \kappa & 0 \\ 0 & \frac{1}{\kappa} \end{pmatrix} \begin{pmatrix} A_j e^{i(\alpha_j x + \beta_j y - \gamma_j z_j)} \\ B_j e^{i(\alpha_j x + \beta_j y + \gamma_j z_j)} \end{pmatrix}, \end{aligned} \tag{30}$$

with $\kappa := e^{-i\gamma_j \delta_j}$. With these equations, we obtain the propagation relation

$$\begin{pmatrix} E_\parallel \\ \frac{\partial E_\parallel}{\partial z} \end{pmatrix}\Big|_{z=z_{j-1}} = \mathfrak{M}_j \begin{pmatrix} E_\parallel \\ \frac{\partial E_\parallel}{\partial z} \end{pmatrix}\Big|_{z=z_j}$$

for the field and its normal flux on the boundaries with the propagation matrix

$$\mathfrak{M}_j := \begin{pmatrix} 1 & 1 \\ -i\gamma_j & i\gamma_j \end{pmatrix} \begin{pmatrix} \kappa & 0 \\ 0 & \frac{1}{\kappa} \end{pmatrix} \begin{pmatrix} 1 & 1 \\ -i\gamma_j & i\gamma_j \end{pmatrix}^{-1}.$$

Now we consider a stack of m parallel layers with the interfaces corresponding to the discrete $z-$values $z_0, z_1 \dots z_m$. Because the tangential component of the electric field (here $E_\parallel$) and its normal derivative are continuous across a plane interface, we obtain the matrix connecting the field above the stack at $z = z_0$ with the field below at $z = z_m$ by simple matrixmultiplication

$$\left.\begin{pmatrix} E_\parallel \\ \frac{\partial E_\parallel}{\partial z} \end{pmatrix}\right|_{z=z_0} = \prod_{j=1}^{m} \mathfrak{M}_j \left.\begin{pmatrix} E_\parallel \\ \frac{\partial E_\parallel}{\partial z} \end{pmatrix}\right|_{z=z_m}$$

In combination with equation (30) and assuming no incident wave from below the grating ($B_S = 0$ in Figure 3), we end up with a linear relation between A_F and B_F.

4.2 TM-modes

For TM-modes the situation is similar. Now the magnetic field is parallel to the layers, and the $z-$ component is zero. Unlike to the TE case in the TM case the tangential magnetic field $H_\parallel$ and $\frac{1}{k_j^2}\frac{\partial H_\parallel}{\partial n}$ have to be continuous across interfaces where $k_j := \omega\nu_j$ is the absolute value of the wavevector with the refractive index of the layer j called ν_j. Now the normal flux $\frac{\partial H_\parallel}{\partial n}$ jumps at the layer-interfaces. This different interfaceconditions can be included by introducing matrices $\mathfrak{D}_{ij}$ describing the behavior on the interface

$$\left.\begin{pmatrix} H_\parallel \\ \frac{\partial H_\parallel}{\partial z} \end{pmatrix}\right|_{z=z_0} = \mathfrak{M}_1\mathfrak{D}_{12}\mathfrak{M}_2\mathfrak{D}_{23}\dots\mathfrak{M}_m \left.\begin{pmatrix} H_\parallel \\ \frac{\partial H_\parallel}{\partial z} \end{pmatrix}\right|_{z=z_m}$$

with

$$\mathfrak{D}_{ij} := \begin{pmatrix} 1 & 0 \\ 0 & \frac{k_i^2}{k_j^2} \end{pmatrix} = \begin{pmatrix} 1 & 0 \\ 0 & \frac{\nu_i^2}{\nu_j^2} \end{pmatrix}.$$

As in the TE-case we are now able to find a relation between the incoming and the outgoing Rayleigh coefficient of the magnetic field, which is equivalent to the relation of the electric Rayleigh coefficients.

Technical remark:
We end up in both, the TE- and the TM-case with a system of two equations

$$\begin{pmatrix} A_F \\ B_F \end{pmatrix} = M \begin{pmatrix} A_S \\ 0 \end{pmatrix}, \tag{31}$$

where M contains the product of all propagation matrices. With this notation we arrive at the notation

$$B_F = \vartheta A_F = \frac{M_{21}}{M_{11}} A_F.$$

The disadvantage of this approach is that for absorbing layers one has to deal with large numbers in the propagation matrices $\mathfrak{M}_j$ and consequently in M, which reduces the accuracy of ϑ. One possibility to work around this problem is to start with an arbitrary value for A_S, for example one. Next we can evaluate the left hand side of equation (31) by multiplying the vector on the right hand side with one propagation matrix after the other. Thus only the ratio of two matrixelements is necessary for the computation of ϑ, we are allowed to normalize the two-component vector after every matrix multiplication, and we can avoid large numbers.

If we choose basis functions of the plane wave testspace below the grating which are either TE or TM, we are able to calculate the factor ϑ linking an unknown belonging to an up-going plane wave with one corresponding to a downgoing wave. The implementation is done by substituting B_F as ϑA_F in the assembly procedure.

5 Numerical results

The numerical results in this section are calculated using finite element code Netgen/Ngsolve of Schöberl (see `http://www.hpfem.jku.at` or [32]). The linear system of equations is solved with the direct solver PARDISO [29, 30].

5.1 Example 1: a lamellar grating

First we study a two dimensional benchmark problem from literature [15, 3]. The grating is lamellar (compare Figure 4) with a period of $1\mu m$ into x-direction. The width of the grooves is $0.5\mu m$ and their depth $1\mu m$. Above the grating we assume vacuum with refractive index one, and below the grating the refractive index is $0.22 + 6.71i$, which represents a highly conducting material. The grating is illuminated by light with a wavelength of $1\mu m$ under an angle of $30°$ to normal incidence. On the left hand side of Figure 4 the transverse component of the electric field is plotted for TE incidence. At the corners of the grating profile we applied a geometric refinement of order one. The geometric refinement was done by using a general coarse mesh, and by cutting off these vertices at a geometric refinement factor of 0.125. For a polynomial order 12 of the testfunctions, which corresponds to 15 849 unknowns, the resulting intensity 0.7342789 of the reflection of order -1 is close to the results of [15, 3].

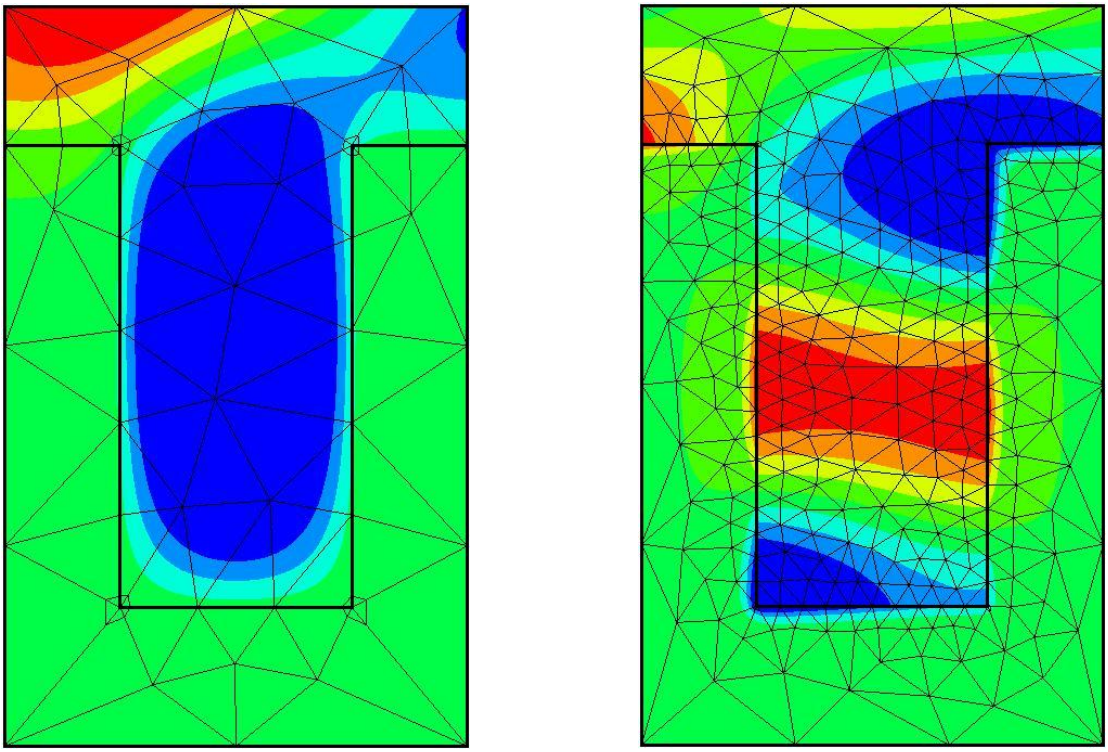

Figure 4: Real part of the electric field for TE modes (left) and the magnetic field for TM modes (right) for example 1

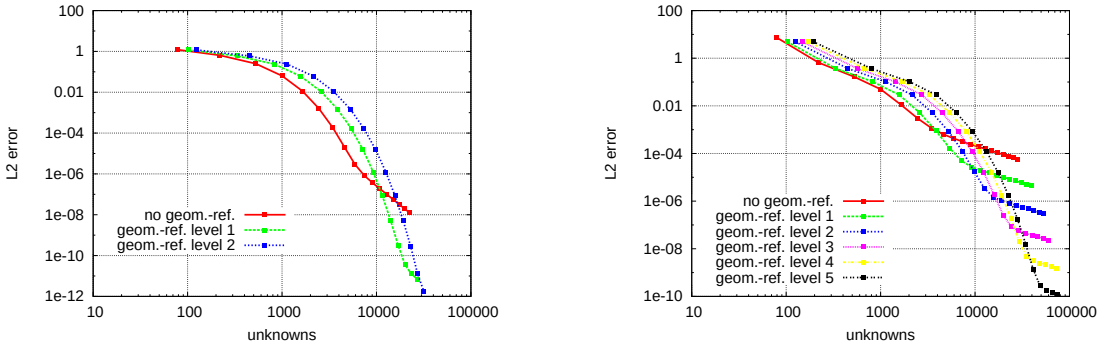

Figure 5: L_2-error as a function of degrees of freedom for the TE- (left) and the TM-case (right) for different levels of geometric refinement in example 1

Due to singularities at the cornerpoints of the grating profile a finer mesh and a geometric refinement of level 5 was used in the TM case. The strong decay of the solution in the absorbing material, which becomes visible on the right hand side of Figure 4, makes it necessary to refine the mesh in this area. For polynomial order 6, which leads to 23 122 degrees of freedom the intensity of 0.8484817 for the zero order reflection is also in good agreement to the results appearing in literature [15, 3].

Next we investigate the dependence of the solution from the number of geometric refinement levels on the cornerpoints of the grating profile and on the polynomial order or the degrees of freedom, respectively. Therefore we calculate the L_2-error by integrating the absolute difference of the actual far-field-solution and a reference solution, calculated with higher accuracy over the boundaries Γ^+ and Γ^-. In Figure 5 the error is plotted as a function of the number of unknowns. The underlying mesh is uniform and the number of degrees of freedom is varied by changing the polynomial order of the testfunctions. Each point in Figure 5 corresponds to a certain polynomial order. The curves show some typical features. In the pre-assymptotic range, at small polynomial orders, the convergence behaves exponentially. Due to a fixed mesh refinement, the rate slows down to algebraic convergence. The left plot of Figure 5 indicates that for TE-modes one level of geometric refinement is sufficient to reach small errors. The situation is different in the TM-case. Because of the singularities in the cornerpoints of the grating profile geometric refinement has a large influence on the error of the solution.

In Figure 6 we consider the dependence of our solution on the position of the artificial interfaces $\Gamma^{\pm}$. For distances of $0.02, 0.1, 0.3$ and $0.6\mu m$ between the boundaries $\Gamma^{\pm}$ and the grating the error is plotted as a function of the number of plane waves used in the calculation. The error is represented by the difference of the zero order

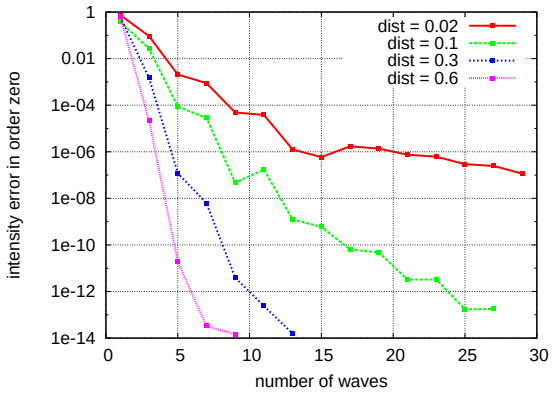

Figure 6: error as function of the number of plane waves for different distances of the boundaries $\Gamma^{\pm}$ of the grating in example 1

reflected intensity and its exact value. Generally we can remark that the smaller the distance between the boundary and the grating, the more basisfunctions are needed to describe the far-field. If the unit cell is cut in a small distance of the grating the local field in the grating influences strongly the field at $\Gamma^{\pm}$, and we have to include apart from two propagating waves a large number of evanescent basis functions. In a large distance we can consider just a few of these evanescent modes, and the far-field can be described almost by propagating waves.

5.2 Example 2: a large unit cell

In this example we examine the same lamellar grating as above, but now the unit cell is chosen much larger than in the last example. In order to show that we are able to treat large two dimensional problems with a small ratio of wavelength to periode, we chose a unit cell consisting of 100 periodes of the grating, while the wavelength is kept constant. For such a grating about 400 plane wave basis functions are needed to describe transmission and reflection. In Figure 7 the field distribution in a part of the unit cell is plotted. The corresponding calculation was performed with a mesh of about 16 000 elements and a polynomial order of 8, which is equivalent to 970 000 unknowns. On a Intel 2 GHz PC the reflected intensities for this geometry were computed with an accuracy up to five digits within 530 seconds.

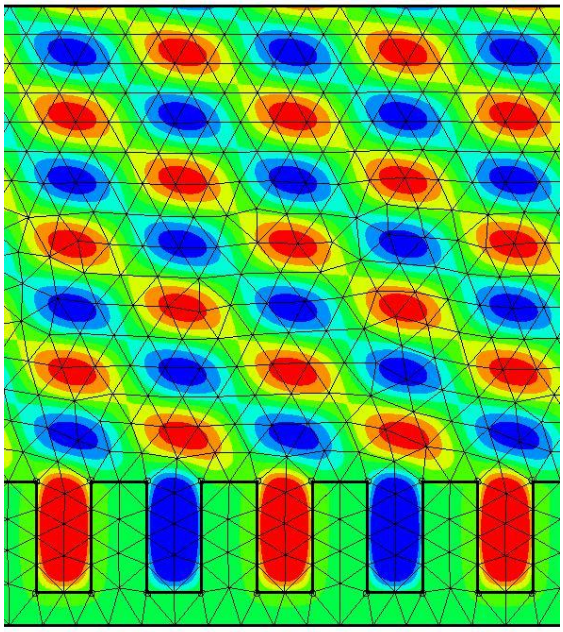

Figure 7: electric field distribution of the supercell in example 2

5.3 Example 3: a three dimensional example

Finally we consider a crossed grating, periodic in x- and y-direction. The unit cell (compare Figure 8) is assumed to have a side length of $0.6\mu m$. The strong absorbing silicon substrate with refractive index $4.76+5.00i$ and a $1\mu m$ thick layer of SiO_2 with refractive index 1.50 (green in Figure 8) are incorporated as substrate layers into the boundary conditions. On top of the SiO_2 is a $0.08\mu m$ thick weakly absorbing layer with refractive index $2.62 + 0.48i$. Into a photoresist (orange in Figure 8) with thickness $0.3\mu m$ and refractive index $1.68 + 0.003i$ cylindric holes with radius $0.15\mu m$ are etched. The refractive index of these holes and the medium above the grating is assumed to be one.
The grating is illuminated by light propagating parallel to the xz-plane under an incident angle of 30°. The electric field is polarized in the xz-plane. In the simulation, we use high order Nédélec finite elements [21, 20, 33, 36, 12], which provide tangential continuous functions and thus they are well suited to satisfy the physical constraint of a tangential continuous electric field. In Figure 8 the real part of the x-component of the electric field distribution for a wavelength of $0.3\mu m$ is plotted. In this picture some physical features can be seen. In the regions with an higher refractive index, like the photoresist (orange), the wavelength is much smaller than above the grating, and the damping of the field in the absorbing layer

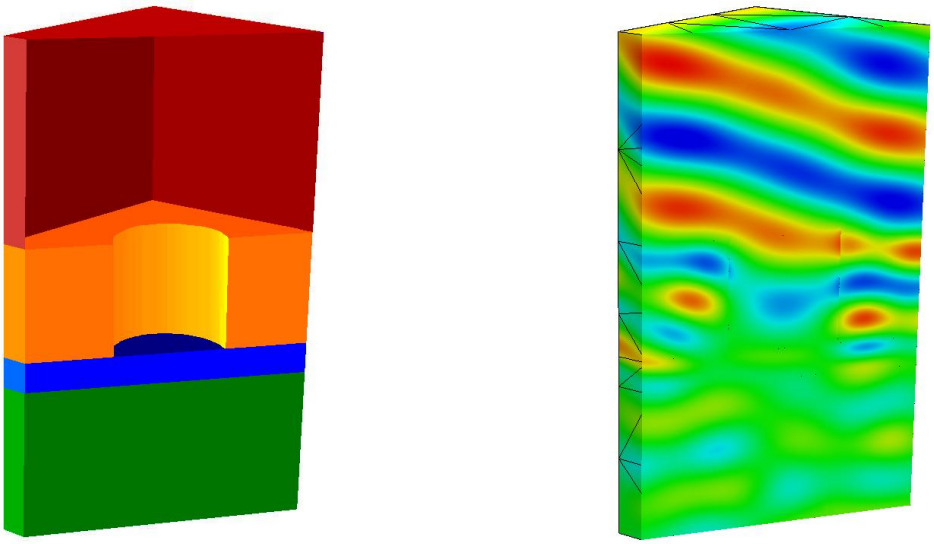

Figure 8: geometry of example 3 and the x-component of the electric field solution

(blue) becomes visible.

For the described setting we vary the wavelength between $0.2\mu m$ and $0.8\mu m$ for different meshes and polynomial orders. The results for the zero order reflected intensity are compared in Figure 9 with a reference solution computed by an RCW code [5]. In the left hand plot the solution for a mesh of 835 elements and a polynomial order of two (which results in 9 100 unknowns) is plotted (green) together with the RCW solution (red). Because of the good agreement between these two curves in the large-wavelength-region the solution can be there approximated for our mesh with small polynomial orders.

For small wavelength the situation is different. In this case we investigated two possibilities to improve our approximation. On the one hand the mesh can be refined, while the polynomial order is kept constant. The blue line on the left hand plot in Figure 9 which was obtained by a finer mesh with 4787 elements and a polynomial order of 2 (about 48 000 unknowns) shows some features of the reference solution, but the approximation is still bad. On the other hand the polynomial order can be increased for the coarse mesh. Using the old mesh and a polynomial order of four, which is equivalent to the number of unknowns used above, we obtain the black line in Figure 9. The black curve seems to be a much better approximation, and for wavelength larger than $0.3\mu m$ it is almost identical to the reference solution (red).

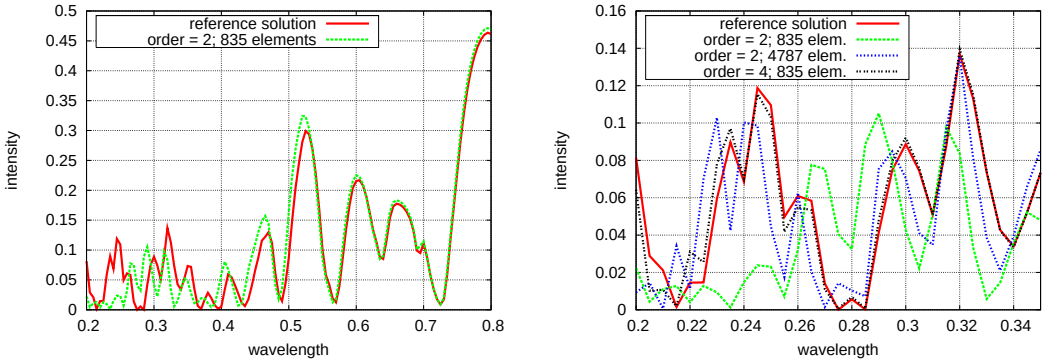

Figure 9: Zero order reflected intensity as a function of wavelength compared with a reference solution for example 3

References

[1] T. Abbound, *Étude mathématique et numérique de quelques problèmes de diffraction d'ondes éléctromagnetiques*, PhD dissertation, Ecole Polytechnique Palaiseau, 1991.

[2] G. Bao, Variational approximation of Maxwell's equations in biperiodic structures, *SIAM J. Appl. Math.*, 57, 2, 364–381, 1997.

[3] G. Bao, Z. Chen and H. Wu, Adaptive finite-element method for diffraction gratings *J. Opt. Soc. Am. A*, 22, 6, 1106–1114, 2005.

[4] G. Bao and D.C. Dobson, On the scattering by a biperiodic structure, *Proc. Am. Math. Soc.*, 128, 2715–2723, 2000.

[5] J. Bischoff, *Beiträge zur theoretischen und experimentellen Untersuchung der Lichtbeugung an mikrostrukturierten Mehrschichtsystemen*, habilitation, TU Ilmenau, Germany, 2001.

[6] F. Bloch, Über die Quantenmechanik der Elektronen in Kristallgittern, *Z. Phys.*, 52, 555–600, 1928.

[7] M. Born and E. Wolf, *Principles of Optics*, 7th edition, Cambridge University Press, 1999.

[8] O.P. Bruno and F. Reitich, Numerical solution of diffraction problems: A method of variation of boundaries, *J. Opt. Soc. Am A*, 10, 1168–1175, 1993.

[9] O.P. Bruno and F. Reitich, Calculation of electromagnetic scattering via boundary variations and analytic continuation, *Appl. Computat. Electromagn. Soc. J.*, 11, 17–31, 1996.

[10] J. Chandezon, M.T. Dupuis, G. Cornet, and D. Maystre, Multicoated gratings: a differential formalism applicable in the entire optical region, *J. Opt. Soc. Am*, 72, 839–846, 1982.

[11] D. Degerfeldt and T. Rylander, A brick-tetrahedron finite-element interface with stable hybrid explicit-implicit time-stepping for Maxwell's equations, *J. Comp. Phys.*, 220, 383–393, 2006.

[12] L. Demkowicz, *Computing with hp Finite Elements. I. One- and Two-Dimensional Elliptic and Maxwell Problems*, CRC Press, Taylor and Francis, 2006.

[13] J. Elschner, R. Hinder and G. Schmidt, Electromagnetic scattering by periodic structures, *Adv. Comp. Math.*, 16, 139–156, 2002.

[14] G. Floquet, Sur les équations différentielles linéaries à coefficients périotiques, *Ann. École. Norm. Sup.*, 12, 47–88, 1883.

[15] G. Garnet, Reformulation of the lamellar grating problem through the concept of adaptive spatial resolution, *J. Opt. Soc. Am. A*, 16, No.10, 2510–2516, 1999.

[16] J.D. Jackson, *Classical Electrodynamics*, 3rd edition, John Wiley & Sons, Inc., 1999.

[17] P. Kuchment, *The Mathematics of Photonic Crystals*, In: Mathematical Modeling in Optical Science,(G. Bao, L. Cowsar, W. Maters, ed.), SIAM Publications, 207–272, 2001.

[18] L. Li, New formulation of the Fourier modal method for crossed surface-relief gratings, *J. Opt. Soc. Am A*, 14, No.10, 2758–2767, 1997.

[19] M.G. Moharam and T.K. Gaylord, Rigorous coupled-wave analysis of planar-grating diffraction, *J. Opt. Soc. Am*, 71, 811–818, 1981.

[20] P. Monk, *Finite Element Methods for Maxwell's Equations*, Numerical Mathematics and Scientific Computation, The Clarendon Press Oxford University Press, 2003.

[21] J.C. Nédélec, A new family of mixed finite elements in $\mathbb{R}^3$, *Num. Math.*, 50, 57–81, 1986.

[22] M. Nevière, G. Cerutti-Maori and M. Cadhilac, Sur une nouvelle méthode de résolution de problème de la diffraction d'une onde plane par un réseau infiniment conducteur, *Opt. Commun*, 3, 48–52, 1971.

[23] E. Nevière and E. Popov, *Light Propagation in Periodic Media: Differential Theory and Design*, Marcel Dekker, New York, 2003.

[24] J. Nitsche, Über ein Variationsprinzip zur Lösung von Dirichlet-Problemen bei Verwendung von Teilräumen, die keinen Randbedingungen unterworfen sind, *Abh. Math. Sem. Univ. Hamburg*, 36, 9–15, 1970/71.

[25] R. Petit (ed.), *Electromagnetic theory of gratings*, Topics in Current Physics, Vol.22, Springer-Verlag, Heidelberg, 1980.

[26] D.W. Prather, M.S. Mirotznik and J.N. Mait, Boundary integral methods applied to the analysis of diffractive optical elements, *J. Opt. Soc. Am A*, 14, 34–43, 1997.

[27] G.A. Reider, *Photonik: Eine Einfhrung in die Grundlagen*, 2nd edition, Springer-Verlag, Wien, 2005.

[28] A. Schädle, L. Zschiedrich, S. Burger, R. Klose and F. Schmidt, *Domain decomposition method for Maxwell's equations: Scattering of oeriodic structures*, ZIB-Report 06-04, Konrad Zuse Institut, Berlin, 2006.

[29] O. Schenk and K. Gärtner, Solving Unsymmetric Sparse Systems of Linear Equations with PARDISO, *Journal of Future Generation Computer Systems*, 20, 3, 475–487, 2004.

[30] O. Schenk and K. Gärtner, On fast factorization pivoting methods for sparse symmetric indefinite systems, *Elec. Trans. Numer. Anal.*, 23, 158–179, 2006.

[31] G. Schmidt, Electromagnetic scattering by periodic structures, *J. Math. Sci.*, 124, 5390–5406, 2004.

[32] J. Schöberl, NETGEN - An advancing front 2D/3D-mesh generator based on abstract rules, *Comput. Visual. Sci.*, 1, 41–52, 1997.

[33] J. Schöberl and S. Zaglmayr, High order Nedelec elements with local complete sequence properties, *COMPEL*, 24, 2, 374–384(11), 2005.

[34] R. Stenberg, Mortaring by a method of J.A. Nitsche, *Computational Mechanics: New Trends and Applications*,(S. Idelsohn, E. Onate, E. Dvorkin, ed.),CIMNE,Barcelona, Spain, 1998.

[35] P. Vincent, A finite-difference method for dielectric and conducting crossed gratings, *Opt. Commun*, 26, 293–296, 1978.

[36] S. Zaglmayr, *High Order Finite Element Methods for Electromagnetic Field Computation*, PhD dissertation, Johannes Kepler Universität Linz, Austria, 2006.